A theoretical study of the interaction between DNA/RNA and the noble metal atoms of gold and silver - Ground-state properties

L. A. Espinosa Leal[1, a)] and O. Lopez-Acevedo[1, b)]
COMP Centre of Excellence, Department of Applied Physics, Aalto University, P.O. Box 11100, 00076 Aalto, Finland

Here, we present results from a study of DNA/RNA bases interacting with gold and silver atoms at three charge states: neutral, cationic, and anionic. Using a real-space DFT methodology, we describe the nature of the stability, bonding, and electronic properties in each hybrid metal. After studying five isolated nucleobases, including the effect of pairing respective DNA-Watson-Crick base pairs and the sugar-backbone by studying the nucleotide guanine monophosphate, we discerned that the energetic ordering of isomers, for a given base-metal combination, follows simple electrostatic rules, and therefore can be extrapolated to more complex structures. When considering the electronic properties of the ground-state structure in every combination of base and charge, we derived several general features. First, allthough the metal localizes almost all of the extra charge in the anionic system, a donation of charge is shared almost equally by the metal and nucleobase in the cationic system. Second, the frontier orbitals of the anionic and cationic system are different, with the latter tending to have more effects from the pairing and inclusion of the backbone. Finally, the electronic gap varies greatly among all of the considered structures and is particularly sensitive to the backbone participation in the bonding. Thus, it could be further used as a fingerprint when searching Au/Ag-DNA hybrid atomic structures.

arXiv:1403.3494v3 [cond-mat.mtrl-sci] 20 May 2014

I. INTRODUCTION

Because of their unique optical properties, stabilized noble metal nanoclusters (MNCs) have gathered a great deal of attention in biochemistry. These nanostructures have the capacity to emit and absorb straightforward electromagnetic radiation in the visible range. This property can be tuned by changing the size (number of atoms), the electronic charge, and/or the surrounding environment. Experimentally, there has been a wide range of stabilizers used, including dendrimers, DNA strands, and water-soluble polymers[1]. Yet, despite the wide interest received and experimental efforts underway, MNCs actual structure is unknown. In addition, cluster fluxionality and a non-covalent metal-organic interaction would allow that isomers close in energy can be attained by thermal agitation. A long-range ordering in the form of crystals therefore can hardly be achieved, and computational support becomes of high necessity in the search for stabilized MNCs atomic structures.

Among the most remarkable stabilizers the DNA/RNA polymers have emerged as a promising bottom-up technology[2]. These hybrid metallic nanostructures present high fluorescent properties upon interaction with few-atom noble metal clusters, in particular gold[3] and silver[4,5]. Recently, an experimental breakthrough has made it possible to measure the composition of DNA-stabilized fluorescent silver clusters[6]. These advances in separation techniques and optical characterization have led to the first identification of numbers of neutral silver atoms, silver ions, and DNA strands contained in fluorescent Ag-DNA complexes. Based on their results, the experimental group has proposed several models of highly charged rod-like structures that would follow a shell (or jellium model) for absorption and emission properties.

To explore this type of shell-structure model with a superatomic electronic counting rule[7] for the metal in DNA/RNA complexes, it is necessary to define an atomic stabilizing layer, a metal core, and to have a set of well-defined electronic properties that the model can explain in a simple way. A guide for this type of exploration, using only ab initio methods, has been presented for metal clusters (of gold, aluminum, and gallium) with different organo-metallic interactions (covalent, ionic, and polarized ionic, respectively)[8].

Previously, several computational studies mainly focused on DNA/RNA-MNCs properties by fixing the charge state or considering a reduced number of nucleobases: search of the structures of the DNA/RNA bases[9], Watson-Crick base pairs[10] interacting with small neutral gold clusters, and single nucleobases interacting with different noble metal atoms[11,12], among others.

In this work, we provide an overview of every possible gold and silver metal atom in DNA/RNA geometries —reporting each atoms corresponding electronic properties as a step towards the modeling of hybrid DNA/RNA-MNCs. We carried out this research using the simplest model of a single nucleobase —guanine (**G**), adenine (**A**), thymine (**T**), cytosine (**C**) and uracil (**U**) —interacting with one noble metal atom (gold and silver) at different charge states (cationic, neutral, and anionic). We studied structural and electronic properties, including ionization potential and electron affinity, Bader charge, electronic gap, and localization of frontier orbitals. For every property, the effects of pairing between bases (Watson-Crick) and the presence of the sugar backbone (guanosine nucleotide) were also simulated and discussed.

a)Electronic mail: leonardo.espinosa@aalto.fi
b)Electronic mail: olga.lopez.acevedo@aalto.fi

II. COMPUTATIONAL METHODOLOGY

We studied the following systems: DNA/RNA nucleobases (see *top* of Fig.1), the DNA Watson-Crick base pairs (see *center* of Fig.1) and one nucleotide with guanine as nucleobase: dGMP (see *bottom* of Fig.1). The work occurred in two parts. In the initial stage, we performed the geometrical global optimizations using the Basin Hopping algorithm[13,14] without any symmetry constraint. A different set of initial configurations were used for each system to find the minimal geometries. In a second stage, we characterized the obtained structures in the ground state: binding energies, electronic gaps, and charge analysis using the Bader method[15]. Moreover, we chose guanine as a benchmark system for testing the choice for the exchange-correlation functional. We compared three charge states with both gold and silver and with different exchange correlations (LDA, PBE, and RPBE). After comparing the final structures and binding energy, we obtained that PBE and RPBE give similar results in terms of structures and type of bond. Thus, the exchange correlation used in all of the calculations in this study is the PBE functional. We detail other results from the comparison in the Appendix.

All calculations in this work have been performed using the DFT code *GPAW*[16,17], which combines real space methods and the projector augmented-wave formalism[18]. We used 8.0 Å of vacuum around the systems in a box-shape simulation box and a real-space grid spacing of 0.18 Å in all simulations. The structure relaxations were performed until the atomic forces were below 0.02 eV/Å. The electronic states H($1s$), C($2s2p$), N($2s2p$), O($2s2p$), Ag($4p4d5s$), Au($5d1s$) were included as valence states, whereas the core states were frozen. The setups were built up, taking into account the relativistic correction for the metal noble atoms.

In the configurational search, a temperature of 1000 K and a maximal step-width of 0.1 Å were combined with the limited-memory Broyden-Fletcher-Goldfarb-Shanno (LBFGS) algorithm[19] as the local optimizer for the Basin Hopping Algorithm. All the RNA/DNA geometries were built using the 3DNA software package[20] and manipulated using Avogadro[21]. The figures of structures and orbitals were plotted using XCrySDen[22].

III. RESULTS AND DISCUSSION

We systematically studied all possible configurations that a noble metal atom (Au and Ag) can form when combined with nucleobases at different charge states (-1, 0, +1). From the bases, we included guanine (**G**), adenine (**A**), thymine (**T**), cytosine (**C**), uracil (**U**), and their respective DNA *Watson-Crick* pairs: guanine-cytosine (**GC**) and adenine-thymine (**AT**), as well as the guanine nucleotide (**dGMP**). All the bases and base pairs have been protonated to replace the sugar backbone. For the guanine nucleotide, apart from the protonation in subsequent and precedent nucleotides, we also protonated the phosphoric group to keep a neutral charge state in the whole system.

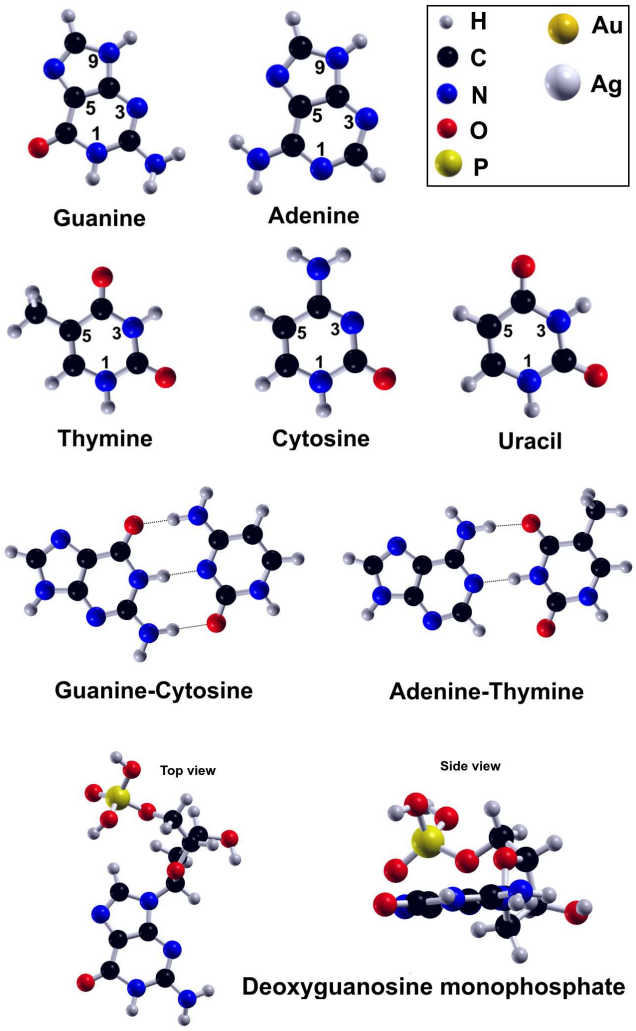

FIG. 1. Structures studied in this work. *Top:* Five protonated nucleobases. Guanine (**G**) and Adenine (**A**) (Purines) and Thymine (**T**), Cytosine (**C**) and Uracil (**U**) (Pyrimidines). *Center*: Protonated DNA *Watson-Crick* base pairs: Guanine-Cytosine (**GC**) (*left*) and Adenine-Thymine (**AT**) (*right*). *Bottom*: Top view (*left*) and side view (*right*) of the guanine nucleotide: Deoxyguanosine monophosphate (**dGMP**). In the top-right box the atomic color convention.

The first step in our research was the choice of the exchange-correlation functional used in all the calculations. We compared the performance of three exchange-correlation functionals: A LDA (PW)[23], GGA (PBE)[24], and an improved version of the revised PBE (RPBE)[25]. The benchmark systems were both the guanine-Au and guanine-Ag structures in all possible configurations at the three charge states (see Supplementary Information). We found that all three approaches predict in the same order the most stable structures. However, LDA tends to overestimate the number of bonding sites. In general, the

local functional predicts a higher-binding energy compared to PBE and RPBE. The comparison between the two GGA functionals shows that RPBE produces better values in the binding energies as opposed to other DFT methodologies, but in general it overestimates the bond length. Meanwhile, the PBE method overestimates the binding energies, but it provides better results for the bond lengths. After carefully reviewing of our results, it was apparent that the binding energies were corrected from PBE to RPBE for a constant value, so then we decided to use PBE for all of our calculations.

A. Structures

The interaction of gold and silver atoms with DNA/RNA nucleobases presents a heterogeneous behavior; however, using our calculations, we extracted an important set of features about the interactions. In general, we can describe the dynamic of the bond between one metallic system and the nucleobases through the analysis of the charge distribution in the molecular structure. In the isolated molecule, the hydrogen present in the imide (N-H), amine (N-H_2), and alkene (C-H) functional groups tends to donate a charge to its bonded atoms, nitrogen and carbon, by following the order of electronegativity: N (3.04) > C (2.55) > H (2.20). Additionally, due to the high electronegativity of oxygen (3.44), this also can act as an important bonding site for the metallic atoms. The redistribution in the electronic potential creates different zones in the nucleobase where the hydrogens behave like positive centers of charge and the rest as negative centers of charge.

This fact defines the dynamics of the interaction of the nucleobase with external charged systems. In general, the binding energies for the systems that interact with silver are much lower than gold; they correlate with a larger bond distance. For most of the obtained hybrid metal-structures, the symmetry was planar, with a few exceptions in the isolated cationic nucleobases —in particular, in the interaction with the silver atoms. More exceptions appear in the cationic base pairs, and when the sugar backbone is considered, the planarity becomes the exception.

Next, we discuss the main structural features obtained from our calculations using a DFT/PBE methodology, ordering the interactions from most to least stable, and listing the preferred binding sites in order of stability (see the most stable hybrid DNA/RNA structures for both gold and silver in the Fig.2 and Fig.3 respectively. For the complete set of structures see the Supplementary Information).

1. Neutral nucleobases

In principle, the neutral metal atom can interact with both the positive and negative centers. The variety of structures and type of bonds in these systems can be explained due to the hybridization of the *s*-orbital with the *d*-orbital in the metal atom (see the orbital analysis in Section III B 4). It allows a redistribution of the electronic cloud that creates an effective dipole moment that interacts with both the positive and negative centers in the molecule. This fact explains in a simple manner the previously reported *non-conventional hydrogen bonds*[9,10] present in the interaction of bare neutral clusters with DNA/RNA nucleobases. The obtained values for the binding energies show that gold atoms are energetically more stable than silver when these interact with the nucleobases. The binding energies for the Au-nucleobase ranges from 13.38-7.70 Kcal/mol (in the most stable structure) obeying the following order **G** > **C** > **A** > **T** > **U**. In the case of Ag-nucleobase, the binding energies ranges from 8.12-3.80 Kcal/mol (in the most stable structure), and they obey the order **C** > **A** > **G** > **T** > **U**.

On average, the binding energies for gold are around twice the values obtained for silver. The bond lengths for the gold-bases are around 0.2 Å shorter than silvers. The first preferred binding sites for the guanine follows the order N3 > N7 > O6 for gold and N7 > O6 > N3 for silver. Additionally, in the case of the bond with the oxygen, there is some interaction with the hydrogen in NH1. The Au-adenine follows the order N1 > N7 > N3, and the Ag-adenine N3 > N1 > N7. The metal-thymine hybrid structures follows the order O4 > O2-NH1 > O2-NH3 for the gold and O2-NH1 > O4 > O2-NH3 for the silver. In cytosine, the preference for the binding sites follows the order N3 > O2-NH1 > O2 for both the gold and silver. The metal-uracil systems obey the order O4-NH3 > O2-NH1 > O4-CH5 > O2-NH3 for the gold and O2-NH1 > O4-NH3 > O4-CH5 > O2-NH3 for the silver.

2. Cationic nucleobases.

When hydrogen is charged positively, it interacts repulsively with the cationic metal. The strong attractive interactions mainly are done through the N and O atoms or in a combination of both when they are adjacent in the molecular structure. This fact can be confirmed by means of the Bader analysis. The binding energy in cationic structures is higher in comparison to the neutral and anionic systems. In the lowest energetic cationic structures, the energy bindings range from 70.78-46.27 Kcal/mol in the hybrid cationic gold-nucleobases and from 68.50-48.16 Kcal/mol in the silver systems. The first case obeys the order **C** > **U** > **A** > **G** > **T** and the second one follows **C** > **G** > **A** > **T** > **U**. The bond lengths in the gold species are, on average, around 0.15 Å shorter than the silver-nucleobase structures. This explains the fact that in the hybrid silver structures, the metal tends to bond with double sites when these are adjacent.

For the cationic systems, we can summarize our results

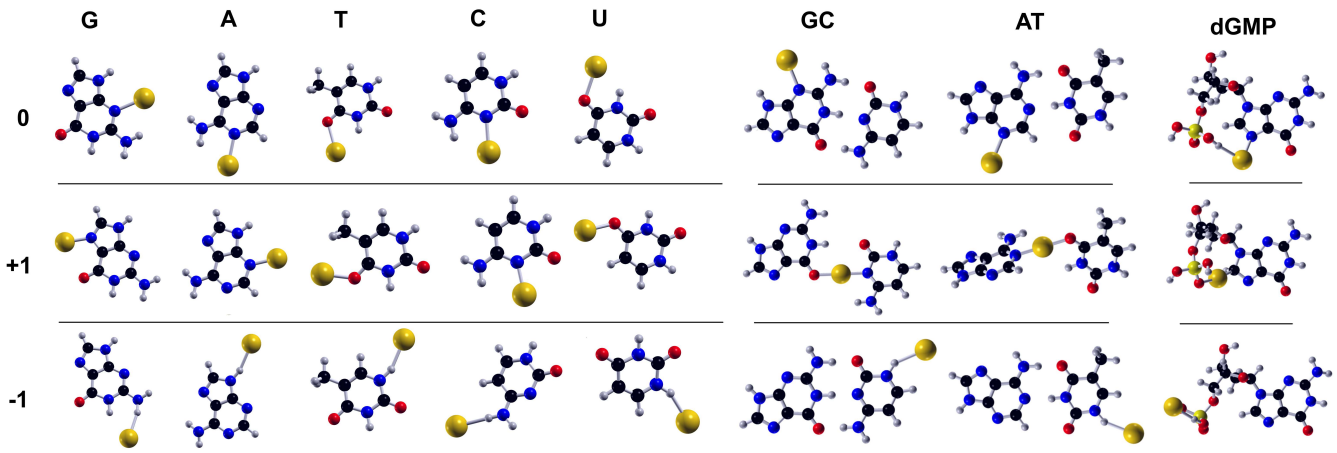

FIG. 2. Most stable hybrid gold-DNA/RNA structures (nucleobases, WC base pairs and deoxyguanosine monophosphate) for the three charge states.

as follows: the binding sites for the cationic gold-guanine systems follow the order N7 > N3 > O6 and for the silver N7-O6 > O6 > N3 > N3 > N1, with these last two lying out of the plane of the molecule. For the gold-adenine, the binding sites obey the order N3 > N1 > N7, which coincides with the binding sites for the silver-adenine systems. In the case of the hybrid gold-thymine structures, the binding sites follow the order O4 > O2 (H3) > O2 (H1) (the sites in parenthesis indicate the orientation, but not a physical-chemical binding), and for the silver-thymine structures, the order O4 (C5) > O2 (H3) > O4 (H3) > O2 (H1). The interaction of the cationic cytosine with the gold metal in the cationic state obeys the order N3 > O2 (N3) > O2 (H1), and in the case of the silver metal, the order is N3-O2 > O2 (H1). For the case of the cationic gold-uracil structures, the binding sites follow the order O4 (H5) > O4 (H3) > O2 (H3) > O2 (H1), and for the hybrid silver-uracil, the order is O4 (H5) > O4 (H3) > O2 (H3) non planar > O2 (H3) > O2 (H1). The binding sites and the order are almost the same, except in the case of silver, when an intermediate non-planar structure appears.

3. Anionic nucleobases.

The interaction of the nucleobases with the gold atom in the anionic system presents a bond length (in average) 0.3 Å shorter than in silver. The binding energy of the most stable structures in gold is around 4 Kcal/mol larger than in the equivalent silver system. The topology of the hybrid metal-nucleobase structures is influenced by the exclusive electrostatic attraction with the hydrogens in the base and the strong repulsion by the O, N, and C atoms. This is because the noble metal is almost totally charged negatively (see the Bader analysis[15]). The order of stability in the metal-base structures is the same for both gold and silver: **G** > **T** > **U** > **C** > **A**. The binding energies range between 26.03-31.28 Kcal/mol for gold and 22.24-28.02 Kcal/mol for silver. For the gold-guanine structures, the binding sites follow the order H2 (H1) > H9 > H2 (N3), and for the silver case, the order of binding is H2-H1 > H9, with a double bond for the most stable in the last case. For the gold-adenine structures, the order of stability is H9 > H6 (N1) > H6 (N7), and for the silver-adenine we have the same first two sites: H9 > H6 (N1). In the thymine-obtained structures, in the case of the interaction with gold, the order of stability in the binding sites follows H3 > H1, and for the interaction with silver, the only place is H3. For the cytosine structures, the binding sites follow the same order for both gold and silver H4 (H5) > H1 > H6 (this last one is a particular structure when the hydrogen is bonded to a carbon atom). In the gold-uracil structures, the order in the binding is H1 > H3, and in the case of the of the silver atom, the only binding site is H1.

4. Watson-Crick Base-pairs.

The effect of pairing between two DNA nucleobases give origin to a big set of stable structures when these interact with a noble metal. This number of structures strongly depends of the charge in the metallic atom, and the structures can form new geometrical distributions. For reference, our results for the binding energies at PBE level for both **GC** and **AT** base pairs are 25.45 Kcal/mol and 13.49 Kcal/mol respectively. The obtained values are in good agreement with other theoretical results obtained using more accurate methodologies such as MP2[26,27] or dispersion-corrected functionals[28,29]. In both hybrid metal base pair structures, the stability for the lowest structure in three charge states follows the rule Au/Ag-**AT** > Au/Ag-**GC**. For the neutral and anionic cases, in the lowest energetic structure, the stability follows the rule **GC** > **AT**, where the most stable structures are those where the metal atom binds far from the binding region between the two nucleobases. For the

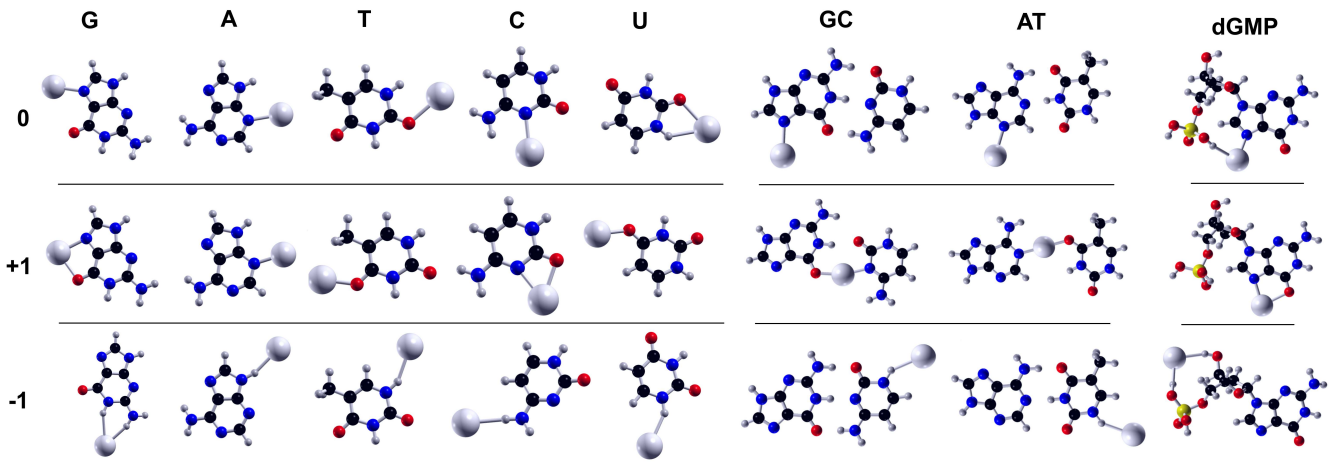

FIG. 3. Most stable hybrid silver-DNA/RNA structures (nucleobases, WC base pairs and guanine monophosphate) for the three charge states.

cationic, the behavior is the opposite and the stability follows **AT** > **GC**, and the most stable structures are those ones where the metal binds between the two nucleobases in the region of the hydrogen bridges. The hybrid neutral gold-**GC** base pair structures obeys the order of stability **G**(N3) > **G**(N7) > **C**(O2-NH1) > **G**(O6) > **G**(O6)-**G**(NH1)-**C**(N3) > **G**(NH2)-**C**(O2). In their silver-equivalent **GC** hybrid structures, the order of stability follows **G**(N7) > **G**(N3) > **C**(O2) > **C**(O2 -non planar-).

A comparison between the Au/Ag-**GC** neutral structures and their equivalent neutral Au/Ag-**G** and Au/Ag-**C** structures show a reduction (with an equivalent increasing in the cytosine) of around 2-3 Kcal/mol in the binding energy when the metal binds the guanine. In the hybrid gold-**AT** neutral structures, the stability obeys the order **A**(N3) > **A**(N7) > **T**(O2-NH1) > **A**(N1)-**T**(NH3) > **T**(O4) > **T**(O2). In the silver equivalent hybrid **AT** structures, the order of stability follows **A**(N3) > **A**(N7) > **T**(O2-NH1) > **T**(O4) > **T**(O2 -non planar-) > **T**(O4 -non planar-). By comparing the results for the Au/Ag-**AT** hybrid system with its individual hybrid structures, we found no appreciable changes in the binding energies.

The hybrid cationic gold-**GC**/**AT** show a similar behavior to its related silvered systems. In both cases, the most stable structures are those ones where the metallic atom lies in between the two nucleobases. Additionally, there are more stable structures in the hybrid silver base pairs than in the gold structures. For the gold-**GC** structures, the order of stability follows the order **G**(O6)-**C**(N3) > **G**(N2)-**C**(N3) > **G**(N7). For the equivalent silver-**GC**, the stability obeys the order **G**(O6)-**C**(N3) > **G**(N7-O6) > **G**(N2)-**C**(O2) > **G**(N3) > **C**(O6) > **G**(O6). If we consider the isolated cationic Au/Ag-**GC** structures in comparison with their individual constituents, we found in the most stable configurations a reduction of around 10 Kcal/mol in the base pair when both metals (gold and silver) bind the guanine nucleobase.

In the hybrid gold-**AT** systems, the most stable structures are not planar, and they obey the stability **A**(N1)-**T**(O4) > **A**(N1-C2)-**T**(O2). In the case of the silver-**AT**, the stability follows the order **A**(N1)-**T**(O4) > **A**(N1)-**T**(O2) > **A**(N6)-**T**(O4) > **A**(N3) > **A**(N7). The pairing effect reduces the binding energy in around 7 Kcal/mol when the gold atom binds the adenine. The anionic structures for both gold and silver atoms interacting with the **GC**/**AT** base pairs behave as the isolated nucleobases, that is, the metal atom binds the base pair only through the hydrogen atoms.

The most stable structures in the hybrid anionic gold-**GC** systems follow the order of stability **C**(NH1) > **C**(NH5-CH6) > **G**(NH9) > **G**(NH2). In the respective silver structures, the order of stability obeys **C**(NH1) > **C**(CH6). The change in the binding energy during the formation of the most stable metallic (gold and silver) anionic **GC** pair (in comparison with the independent parts) is an increase of around 5 Kcal/mol in the cytosine and its respective loss in the guanine. In the anionic gold-**AT** structures, the order of stability is as follows: **T**(NH1) > **A**(NH9) > **A**(NH6), and the respective order for the silver structures **T**(NH1) > **T**(CH6). In this case, the variation in the energy binding due to pairing effect is less than 2 Kcal/mol for both metals (gold and silver).

5. Deoxyguanosine monophosphate

The inclusion of the sugar backbone in the metal-guanine system brings new possible configurations. In the case of the neutral system, among the most stable structures are a set that is similar to the structures in the isolated metal-guanine case. In the most stable neutral structure for both metals, gold and silver bind the N7 site with the OH functional group. The stability in

the gold case for the planar structures obeys the order N3 > N7 > O6, and for the silver N7 > N3 > O6 (we changed the order with respect to the isolated neutral Ag-guanine). The change in the energy binding in the comparable cases is a maximum of around 1 Kcal/mol less when the sugar backbone is considered.

In the cationic structures, the planarity is less favored due to a strong interaction of the metal with the oxygen atoms present in the phosphoric groups in the sugar backbone. In the cationic gold-**dGMP**, the most stable structure is non-planar, and the order of stability follows N7 > N3 > O6. For the silver-**dGMP**, the most stable structure is planar and coincides with the isolated cationic silver-guanine N7-O6; the rest are non-planar structures. For gold, the inclusion of the backbone in the cationic systems increases the binding energy by around 3-4 Kcal/mol, but it remains constant for silver. In the anionic case, in both metals a stronger interaction occurs with the OH functional groups present in the backbone. A comparison with the equivalent isolated cases shows that the binding energy for gold increases around 7-8 Kcal/mol when the sugar backbone is included; meanwhile, in silver, it remains almost constant.

B. Ground state electronic properties

1. Ionization Potential and Electron Affinity

In the study of electronic properties of charged systems, it is important to start by calculating the Ionization Potential (IP) and Electron Affinity (EA) of the different species. The EA lets us estimate the anionic system, in which the two subsystems will most likely accept the extra charge. Using the IP, on the other hand, it is possible to estimate a possible charge redistribution during the cation's formation.

In Table I, we present the results in the calculation of the adiabatic, vertical IP, and EA as total energy differences, and also from the energy of the highest occupied orbital for the DNA/RNA nucleobases, DNA base pairs, and the gold and silver atoms. The quantities were calculated using the definitions EA=E(N)-E(N+1) for the electron affinity and IP=E(N-1)-E(N) for the ionization potential. Here, E(N) is the total ground-state energy of the neutral system and E(N+1) and E(N-1) the total energy in the same anionic (after adding one electron) or cationic (after removing one electron) system.

From the simulation, we can see that the EA of the metals is higher than all the nucleobases and base-pairs. The results indicates then that the metal atom (Au/Ag) has a tendency to capture the electron during the formation of the anionic base-metal and pairs-metal structures.

The experimental values as well other theoretical calculations are all very close, with EA of metals higher than all the nucleobases, except for the EA of guanine, which can be smaller than Ag.

The subsystem with the lowest IP would most likely donate an electron to the bonded system. From the simulation gold and silver have opposite characteristics. While the IP of Au is higher than all the nucleobases, the IP of Ag is smaller than all of them with, the exception of guanine. From the simulated IP, we expect to see that in the cation's formation, the nucleobase loses one electron when bonded to Au. However, in the case of the Ag, we expect the opposite that the metal would lose the electron, again with the exception of guanine. In the experiment, the same trend is observed (the IP of Au higher than the IP of the nucleobases and the IP of Ag smaller than the IP of the nucleobases), however there is no exception from guanine.

2. Bader charge

As expected from the high values of the EA of the metals in the case of the anionic metal-nucleobase structures, there is a large electronic density accumulated in the metal atom. The Bader charge varies only a little among all obtained single and paired structures (from -0.8 $|e|$ to -0.9 $|e|$, see Table II). The extra charge present in the total system is practically localized in the metal atom.

In the cationic case, the missing electronic charge density is removed mainly from the metal atom. However, important variations reflect the difference in the IP of Au and Ag. The positive Bader charge of Au is smaller than the positive Bader charge of Ag (it varies from 0.4 $|e|$ to 0.6 $|e|$, and from 0.7 $|e|$ to 0.8 $|e|$, respectively). No exceptional value is found in guanine, despite a different simulated IP. In the cationic case, even if most of the electronic charge is removed from the metal, there is an important contribution from the nucleobase. A trend is observed, wherein the metal retains a higher charge (in anion) or loses less charge (in cation) when the metal-nucleobase bond involves a single oxygen atom; this explains the Bader's variability for a given nucleobase. The structures with the oxygen-metal bond are formed with the thymine and uracil nucleobases.

In the neutral system, almost no charge is present in the formed metal-nucleobase, in accordance with the very low binding energy. A small negative Bader charge is present in the metal atom in the neutral metal-nucleobases structures.

The system that includes **AT** and **GC** base pairs have a similar metal atom Bader charge, again with variations of the order of 0.1 $|e|$. In the anionic case, the metal is bound to one of the pairs, and the Bader charge is -0.8 $|e|$ and 0.9$|e|$ for Ag and Au, respectively. In the cation, the metal has a Bader charge of 0.6 $|e|$ and 0.4 $|e|$ for Ag and Au.

The addition of backbone to the system guanine-metal changes the Bader charge by 0.2 $|e|$ in the most extreme case. The metal accumulates most of the charge in the anionic case, and the Bader charge is -0.7 $|e|$ for both Au and Ag, but this is smaller in absolute value than the

TABLE I. Adiabatic Ionization Potential (IP_a), vertical Ionization Potential (IP_v), Koopmans's ionization potential (IP_k), adiabatic electron affinity (EA_a), vertical electron affinity (EA_v) and Koopmans's electron affinity (EA_k) for the DNA/RNA nucleobases, WC Base Pairs, guanosine monophosphate and transition metals (gold and silver).

Str.	IP_a	IP_v	IP_k	IP_{exp}	EA_a	EA_v	EA_k	EA_{exp}
G	7.58	7.86	5.31	7.77 to 7.85[a], 8.0 to 8.3[b]	-0.027	0.069	1.44	-0.44[e], -2.07 to -0.08[f]
	7.81[c], 7.51[d]	8.05[c],7.80[d]	5.45[c],5.27[d]		-0.049[c],-0.025[d]		1.54[c],1.43[d]	
A	8.00	8.16	5.54	7.80 to 8.55[a], 8.3 to 8.5[b]	-0.279	0.317	1.72	-0.72[e],-0.56 to -0.45[f]
T	8.61	8.78	6.05	8.80 to 8.87[a], 9.0 to 9.2[b]	-0.043	0.058	2.30	0.02-0.068[e],-0.53 to -0.29[f]
C	8.63	8.59	5.73	8.45 to 8.68[a], 8.8 to 9.0[b]	-0.107	0.187	2.06	-0.10[e],-0.55 to -0.32[f]
U	9.11	9.22	6.29	9.20 to 9.32[a], 9.4 to 9.6[b]	-0.079	0.018	2.46	0.03[e],-0.30 to -0.22[f]
GC	6.82	7.11	4.82	7.05,7.50[g]	0.184	-0.184	2.42	-0.48[h]
AT	7.43	7.53	5.46	7.85,8.27[g]	0.287	-0.179	2.19	-0.18 [h]
dGMP	7.32	7.75	5.33	7.96[i]	0.31	0.24	1.52	0.24,0.14[j]
Au	9.54	-	6.03	9.23[k]	2.25	-	0.84	2.31[k]
Ag	7.91	-	4.70	7.58[k]	1.22	-	0.78	1.30[k]

[a] Experimental adiabatic values in TABLE IV. in Ref[30].
[b] Experimental vertical values in TABLE I. in Ref[30].
[c] with LDA.
[d] with RPBE.
[e] Theoretical adiabatic values in TABLE III. in Ref[31] from CASPT2(IPEA)/ANO-L 4321/ 321//CCSD/ aug-cc-pVDZ calculations.
[f] Experimental vertical values in TABLE II. in Ref[31] except for guanine where the values are from the B3LYP range.
[g] ZPE corrected M06-2X/6-31++G(d,p). TABLE II in Ref[32]
[h] ZPE corrected M06-2X/6-31++G(d,p). TABLE I in Ref[32]
[i] Vertical IP at MP2/6-311G(d,p)//P3/6-311G(d,p) level. TABLE III in Ref[33]
[j] Adiabatic and vertical values at B3LYP/DZP++ level. TABLE I in Ref[34]
[k] from Ref[35]

Ag-**G** alone by 0.2 $|e|$. Indeed, the bonding configuration is completely different with the backbone atoms participating in it. In the case of the cation, Ag has the same Bader charge, but Au has a Bader charge of 0.3 $|e|$ that is 0.2 $|e|$ lower than Ag-**G** alone. Again, the configurations are different with participation of the backbone atoms in the bonding.

3. Electronic HOMO-LUMO gap

The HOMO-LUMO gap varies importantly among the structures. We therefore can expect a high dependence on the system's optical properties to discern the metal-attaching site inside a DNA strand. Not all cases could be (in principle) distinguished by the use of the electronic gap, but it will be a powerful tool as a guide to rule out configurations.

For a given metal, the simplest case to consider is the anion. The HOMO-LUMO gap of the formed Au-nucleobases is 1.7-1.8 eV in the case of the single bases (**A**, **T**, **C**, **U**). The Au-guanine gap is strikingly different (2.23 eV), it is reduced by 0.1 eV when the backbone participates in **dGMP** system. In the case of metal bonded to the pair **AT**, the gap is reduced considerably (by 0.6 eV) with respect to the corresponding Au-nucleobases.

The same trend is valid for silver. The Ag-**G** gap is the highest (1.35 eV), reduced by 0.2 eV with regard to participation of backbone. All the other Ag-nucleobases (**A**, **T**, **C**, **U**) have a similar gap, but they are more spread out than the Au case (from 0.80 to 0.94 eV). In the instance where Ag is bonded to the pair **AT**, the gap is again reduced considerably (by more than 0.6 eV) with respect to the corresponding Ag-nucleobases. In the anion case, the systems's gaps are smaller when the metal is Ag than it is with Au.

In the case of the cation, the reverse is observedthe Ag-bases gap is higher than the Au-bases gap. The electronic gap in the Au-pair system varies greatly for the single bases (from 1.23 eV to 1.94 eV). The case of metal bonded to the pair **GC** and **AT** changes the gap. It is increased considerably (by more than 0.5 eV and 0.7 eV for **GC** and **AT**, respectively). Including the backbone in the bonding to the Au also drastically changes the electronic gap. Ag-**G** changes from 1.23 eV to 2.26 eV in **dGMP**. The case of the cation and Ag is similar when considering the gap variability within the single bases (from 1.49 to 2.81 eV). The gap in the metal-nucleobase pairs is completely different than the single ones. Contrary to Au, the inclusion of backbone does not significantly change the gap between M-**G** and **dGMP**.

4. HOMO-LUMO orbitals

The form of the frontier orbitals has the expected shape, following the analysis of the Bader charge. The shape of the orbitals for the different bases and metals are similar, and we include the adenine case in Figure 4 as a reference.

TABLE II. Bader analysis on the metal atom (in e units): gold and silver (and HOMO-LUMO gap) neutral[a] for the most stable DNA/RNA hybrid metal structures obtained at PBE level.

	Gold (79)			Silver (47)		
System	neutral	cation	anion	neutral	cation	anion
G	-0.2 (2.05/2.65)	0.5 (1.23)	-0.8 (2.23)	-0.1 (3.28/1.23)	0.7 (2.30)	-0.9 (1.35)
A	-0.2 (2.43/1.86)	0.4 (1.28)	-0.9 (1.80)	-0.1 (3.20/1.28)	0.7 (1.49)	-0.9 (0.94)
T	-0.1 (1.86/1.85)	0.6 (1.31)	-0.8 (1.77)	0.0 (2.88/1.60)	0.8 (1.70)	-0.8 (0.88)
C	-0.2 (2.43/1.22)	0.5 (1.94)	-0.9 (1.71)	-0.1 (3.27/0.67)	0.7 (2.81)	-0.9 (0.80)
U	-0.1 (1.85/1.75)	0.6 (1.57)	-0.8 (1.77)	0.0 (2.91/1.62)	0.8 (1.96)	-0.8 (0.83)
GC	-0.2 (2.01/1.49)	0.4 (2.47)	-0.9 (1.64)	-0.1 (2.63/0.33)	0.6 (1.87)	-0.8 (0.71)
AT	-0.2 (2.40/1.63)	0.4 (3.06)	-0.9 (1.11)	-0.1 (3.11/1.14)	0.6 (3.12)	-0.8 (0.29)
dGMP	-0.1 (2.26/2.25)	0.3 (2.26)	-0.7 (2.11)	0.0 (2.82/1.71)	0.7 (2.24)	-0.7 (1.12)

[a] For neutral systems with HOMO-SOMO/SOMO-LUMO gaps.

TABLE III. Electronic HOMO-LUMO[a] gaps of all DNA/RNA hybrid metal structures studied in this work (from the most to the least stable) at the PBE level.

	Au			Ag		
System	neutral	cation	anion	neutral	cation	anion
G	2.05, 2.28, 1.77, 1.56, 0.35, 0.25	1.23, 0.56, 0.43	2.23, 1.61, 1.92	3.28, 2.43, 2.45, 0.67	2.30, 0.80, 0.93, 0.82, 0.71	1.35, 0.74
A	2.43, 2.43, 2.41,	1.28, 1.26, 0.81	1.80, 1.28, 1.48	3.20, 3.19, 2.95	1.49, 1.51, 1.12	0.94, 0.47
T	1.86, 1.80, 1.78, 0.58	1.31, 0.81, 0.97	1.77, 0.96	2.88, 3.12, 3.00	1.70, 1.04, 1.44, 1.28	0.88
C	2.43, 1.94, 1.72,	1.94, 1.95, 1.57	1.71, 1.69, 1.41	3.27, 3.02, 3.09	2.81, 1.91	0.80, 0.81, 0.48
U	1.85, 1.76, 1.73, 1.76	1.57, 1.37, 0.91, 1.11	1.77, 0.93	2.91, 3.10, 3.15, 3.08	1.96, 1.79, 1.31, 1.40, 1.33	0.83
GC	2.01, 2.32, 0.94, 1.67, 3.43, 1.33	2.47, 2.40, 0.75	1.64, 1.35, 1.09 0.37	2.63, 2.39, 1.59, 1.72	1.87, 1.72, 3.45, 0.66, 0.03, 0.15	0.71, 0.31
AT	2.40, 2.45, 1.58, 2.39, 1.60, 1.55	3.06, 2.01	1.11, 1.09, 0.25	3.11, 2.95, 2.23, 2.33, 2.44, 1.93	3.12, 3.53, 3.40, 0.44, 0.12	0.29, 0.08
dGMP	2.26, 1.75, 1.58, 2.28, 1.79, 1.70	2.26, 1.21, 2.12, 1.51, 0.69, 0.61	2.11, 2.04, 1.69, 1.71, 1.61, 1.22	2.82, 3.29, 2.22, 2.42, 1.86,	2.24, 2.20, 2.62, 2.32, 1.44	1.12, 1.20, 0.87, 0.76,0.59, 0.42

[a] For neutral systems the HOMO-SOMO gap.

In the case of the anions, the extra electronic charge is highly localized in the metal. The HOMO of the anionic case is also localized in the metal, and corresponds as expected to the metals closed $5s$ or $6s$ electronic shell. The anionic system's LUMO is in all cases the LUMO of the non-bonded nucleobase.

In the case of the cationic system, the electronic charge is donated by both subsystems metal and the nucleobase. Correspondingly, the form of the LUMO in the cationic case is an electron delocalized between the metal and the nearest atom(s) in the nucleobase forming the bond. Because there are different types of atoms in the bond between the structures, this explains the variability of the electronic gap. The HOMO of the cationic system is the HOMO of the non-bonded nucleobase.

When forming the pairs (see Figure 5), the HOMO of the anion remains localized in the metal and LUMO in one of the bases. In the pair **AT**, while the metal binds to **T**, the LUMO is localized in **A**. The opposite appears in the **GC** pair. The metal binds to **C**, but the LUMO is localized in **C**. In the cation, where the metal is binding simultaneously both bases in the pair, the HOMO and LUMO are localized in the bases. In the **GC** pair, HOMO is in **G** while LUMO is in **C**; and in the **AT** pair, HOMO is in **A**, while LUMO in **T**.

The anion system that includes the backbone has the same HOMO and LUMO as the metal-base alone (see Figure 6). The cation case, however, is quite different, as would be expected from a new configuration that includes a bond between the metal and atoms in the backbone. The HOMO is delocalized between the metal and the base (it was only on the base in absence of the backbone), and the LUMO is also an orbital delocalized between the metal and the base. Depending on the case, the HOMO-LUMO transition is expected to have a low or high oscillatory strength in optical absorption. A complete analysis of the other orbitals, along with their relation to bonding and optical properties, will be reported in a following study.

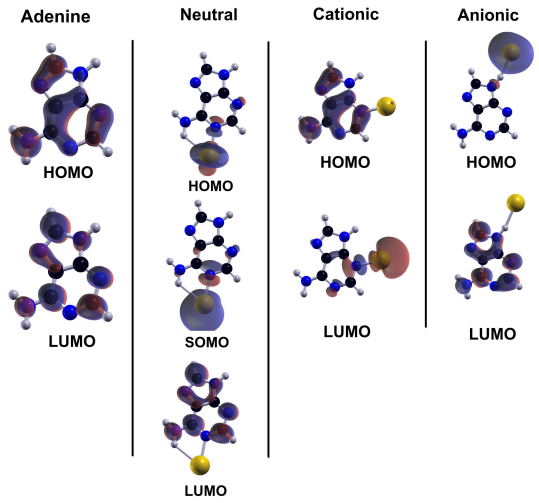

FIG. 4. Representative HOMO-LUMO Kohn-Sham Orbitals for the isolated adenine (**A**) nucleobase (on the *left*) and its lowest energetic gold hybrid structures in three charge states: neutral, cationic, and anionic.

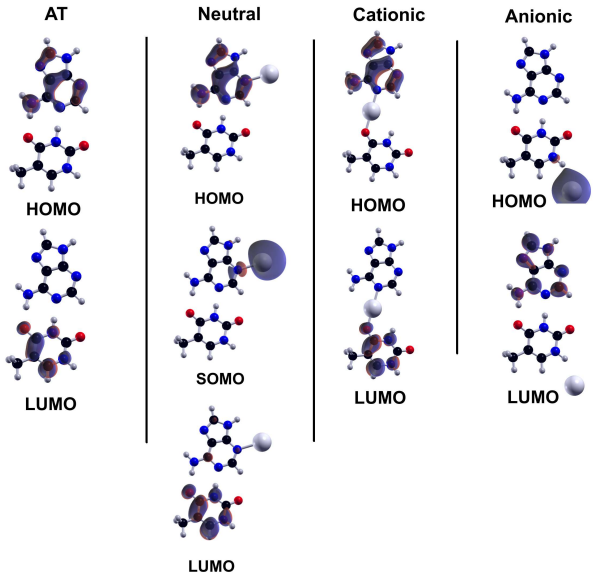

FIG. 5. Representative HOMO-LUMO Kohn-Sham Orbitals for the isolated adenine-thymine (**AT**) base pair (on the *left*) and its lowest energetic silver hybrid structures in three charge states: neutral, cationic, and anionic.

IV. CONCLUSIONS

Our results provide an exhaustive study of the interaction, stability, and electronic properties of the DNA/RNA nucleobases interacting with the noble metal atoms (gold and silver) in three charge states: cationic, neutral, and anionic using a DFT real-space methodology implementation. We have taken into account the paring effect by studying the Watson-Crick base pairs and by including the sugar-backbone in the guanine nucleobase.

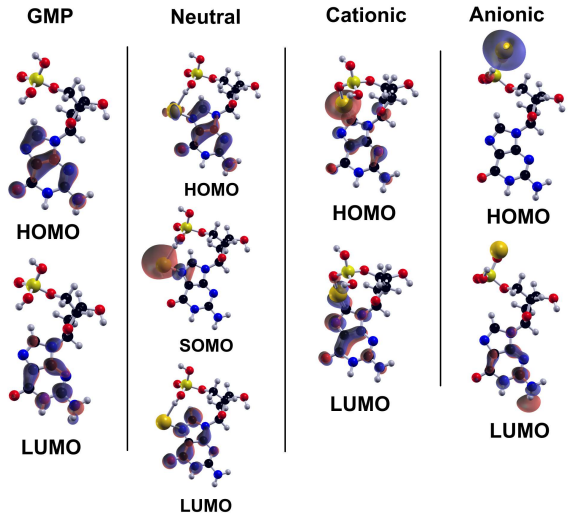

FIG. 6. Representative HOMO-LUMO Kohn-Sham Orbitals for the isolated guanine monophosphate (**dGMP**) structure (on the *left*) and its lowest energetic gold hybrid structures in three charge states: neutral, cationic, and anionic.

We found that the hybrid metal structures topology is dominated by an electronic redistribution of charges in the molecule. In general, nitrogen, oxygen, carbon, and phosphorus behave as negative centers, while hydrogen behaves as a positive center. For anions and cations, the bonding energy of the metal-base increases as the Bader charge of the atom base increases, and the bonding energy decreases when atoms that are opposite charge centers are present. The Bader analysis showed that the gain in electronic charge is mainly localized on the noble metal atom for anions. For cations, the electronic charge is donated partially by the metal and partially by the nucleobase (so the donation charge is shared almost equally).

In the neutral case, binding occurs through positive and negative centers, where the s electronic orbital in the metal atom hybridizes with the d orbital by redistributing the charge to favor the dipolar interaction. For the anionic case, the orbital analysis of frontier orbitals is also homogenous. The HOMO orbitals are localized in the metal and the LUMO are localized in the nucleobase, with no change induced by the inclusion of the backbone or pairing. In the cationic case, the HOMO is localized in the base, and also in the backbone when included, while the LUMO is delocalized between the metal and base. When considering pairs, HOMO and LUMO are each localized in a different nucleobase. Finally, the electronic gap varies greatly among all of the considered structures, and is particularly sensitive to the backbone participation in the bonding. Thus, it could be used as a fingerprint when searching Au/Ag-DNA hybrid atomic structures.

ACKNOWLEDGMENTS

We gratefully acknowledge financial support from the Centre of Excellence in Computational Nanoscience (COMP); and we are grateful to CSC, the Finnish IT Center for Science in Espoo, for computational resources.

[1] L. Shang, S. Dong, and G. U. Nienhaus, Nano Today **6**, 401 (Aug. 2011).
[2] G. Doria, J. Conde, B. Veigas, L. Giestas, C. Almeida, M. Assunção, J. Rosa, and P. V. Baptista, Sensors **12**, 1657 (2012).
[3] G. Liu, Y. Shao, K. Ma, Q. Cui, F. Wu, and S. Xu, Gold Bulletin **45**, 69 (2012).
[4] H.-C. Yeh, J. Sharma, I.-M. Shih, D. M. Vu, J. S. Martinez, and J. H. Werner, Journal of the American Chemical Society **134**, 11550 (Jul. 2012).
[5] K. Morishita, J. L. MacLean, B. Liu, H. Jiang, and J. Liu, Nanoscale **5**, 2840 (2013).
[6] D. Schultz, K. Gardner, S. S. R. Oemrawsingh, N. Markeevi, K. Olsson, M. Debord, D. Bouwmeester, and E. Gwinn, Advanced Materials **25**, 27972803 (2013), ISSN 1521-4095.
[7] M. Walter, J. Akola, O. Lopez-Acevedo, P. D. Jadzinsky, G. Calero, C. J. Ackerson, R. L. Whetten, H. Grnbeck, and H. Hkkinen, Proceedings of the National Academy of Sciences **105**, 9157 (2008).
[8] O. Lopez-Acevedo, P. A. Clayborne, and H. Häkkinen, Phys. Rev. B **84**, 035434 (Jul 2011).
[9] E. S. Kryachko and F. Remacle, Nano Letters **5**, 735 (2005).
[10] E. S. Kryachko and F. Remacle, The Journal of Physical Chemistry B **109**, 22746 (2005), pMID: 16853964.
[11] A. Martínez, The Journal of Chemical Physics **123**, 024311 (2005).
[12] J. Valdespino-Saenz and A. Martínez, The Journal of Physical Chemistry A **112**, 2408 (2008).
[13] D. J. Wales and J. P. K. Doye, The Journal of Physical Chemistry A **101**, 5111 (1997).
[14] D. J. Wales and H. A. Scheraga, Science **285**, 1368 (1999).
[15] W. Tang, E. Sanville, and G. Henkelman, Journal of Physics: Condensed Matter **21**, 084204 (2009).
[16] J. J. Mortensen, L. B. Hansen, and K. W. Jacobsen, Phys. Rev. B **71**, 035109 (Jan 2005).
[17] J. Enkovaara, C. Rostgaard, J. J. Mortensen, J. Chen, M. Duak, L. Ferrighi, J. Gavnholt, C. Glinsvad, V. Haikola, H. A. Hansen, H. H. Kristoffersen, M. Kuisma, A. H. Larsen, L. Lehtovaara, M. Ljungberg, O. Lopez-Acevedo, P. G. Moses, J. Ojanen, T. Olsen, V. Petzold, N. A. Romero, J. Stausholm-Møller, M. Strange, G. A. Tritsaris, M. Vanin, M. Walter, B. Hammer, H. Häkkinen, G. K. H. Madsen, R. M. Nieminen, J. K. Nørskov, M. Puska, T. T. Rantala, J. Schiøtz, K. S. Thygesen, and K. W. Jacobsen, Journal of Physics: Condensed Matter **22**, 253202 (2010).
[18] P. E. Blöchl, Phys. Rev. B **50**, 17953 (Dec 1994).
[19] D. Liu and J. Nocedal, Mathematical Programming **45**, 503 (1989), ISSN 0025-5610.
[20] X. Lu and W. K. Olson, Nucleic Acids Research **31**, 5108 (2003).
[21] M. Hanwell, D. Curtis, D. Lonie, T. Vandermeersch, E. Zurek, and G. Hutchison, Journal of Cheminformatics **4**, 1 (2012).
[22] A. Kokalj, Journal of Molecular Graphics and Modelling **17**, 176 (1999), ISSN 1093-3263.
[23] J. P. Perdew and Y. Wang, Phys. Rev. B **45**, 13244 (Jun 1992).
[24] J. P. Perdew, K. Burke, and M. Ernzerhof, Phys. Rev. Lett. **77**, 3865 (Oct 1996).
[25] B. Hammer, L. B. Hansen, and J. K. Nørskov, Phys. Rev. B **59**, 7413 (Mar 1999).
[26] N. Kurita, V. I. Danilov, and V. M. Anisimov, Chemical Physics Letters **404**, 164 (2005), ISSN 0009-2614.
[27] J. Šponer, P. Jurečka, and P. Hobza, Journal of the American Chemical Society **126**, 10142 (2004), pMID: 15303890.
[28] F. Hanke, Journal of Computational Chemistry **32**, 1424 (2011).
[29] E. G. Hohenstein, S. T. Chill, and C. D. Sherrill, Journal of Chemical Theory and Computation **4**, 1996 (2008).
[30] D. Roca-Sanjuán, M. Rubio, M. Merchán, and L. Serrano-Andrés, The Journal of Chemical Physics **125**, 084302 (2006).
[31] D. Roca-Sanjun, M. Merchn, L. Serrano-Andrs, and M. Rubio, The Journal of Chemical Physics **129**, 095104 (2008).
[32] Y. Paukku and G. Hill, The Journal of Physical Chemistry A **115**, 4804 (2011).
[33] D. M. Close and K. T. Øhman, The Journal of Physical Chemistry A **112**, 11207 (2008).
[34] J. Gu, Y. Xie, and H. F. Schaefer, Nucleic Acids Research **35**, 5165 (2007).
[35] D. Lide, *CRC Handbook of Chemistry and Physics, 84th Edition*, CRC HANDBOOK OF CHEMISTRY AND PHYSICS (Taylor & Francis, 2003).